Performance of steel reinforcement in Portland cement and high-volume fly ash concretes exposed to chloride solution

Gu, P.; Beaudoin, J. J.; Zhang, M. H.; Malhotra, V. M.

Publisher's version / Version de l'éditeur:

ACI Materials Journal, 96, Sept-Oct. 5, pp. 551-558, 1999-09-01

Performance of steel reinforcement in Portland cement and high-volume fly ash concretes exposed to chloride solution

NRCC-42641

Gu, P.; Beaudoin, J.J.; Zhang, M.H.; Malhotra, V.M.

September 1999

A version of this document is published in / Une version de ce document se trouve dans:
ACI Materials Journal, 96, (5), Sept-Oct., pp. 551-558, September 01, 1999

Title no. 96-M68

Performance of Steel Reinforcement in Portland Cement and High-Volume Fly Ash Concretes Exposed to Chloride Solution

by Ping Gu, J. J. Beaudoin, Min-Hong Zhang, and V. M. Malhotra

This paper describes the performance of steel reinforcement in portland cement and high-volume fly ash (HVFA) concretes exposed to a chloride solution. A number of large slabs, 833 x 600 x 153 mm in size, were cast from six air-entrained concrete mixtures. Four of these mixtures were made with normal portland cement with the water-cement ratio (w/c) of the mixtures ranging from 0.32 to 0.76; the remaining two mixtures were made with the HVFA concrete with a w/(c + FA) of 0.32. The steel reinforcing bars were placed in concrete with cover thickness ranging from 13 to 76 mm. The concrete slabs were ponded with a 3.4% sodium chloride solution for a period of 6 months, and half-cell potential, linear polarization, and AC impedance techniques were applied to monitor the progress of the corrosion of steel reinforcement.

The results indicate that the performance of the reinforcing steel bars in the HVFA concrete after 6 months of ponding with a 3.4% sodium chloride solution was excellent. There was no significant steel corrosion taking place on the reinforcing bars embedded in the HVFA concrete, even with 13 mm concrete cover. This performance of the HVFA concrete is equivalent to that of the control concrete with a w/c of 0.32, and is better than the control concrete with w/c ≥ 0.43.

Significant corrosion rates were observed for the reinforcing bars embedded in control portland cement concrete with w/c ≥ 0.43. As expected, the poorest performance was of the control concrete with a w/c of 0.76, where even the reinforcing bars with 51 mm cover exhibited corrosion.

Keywords: chlorides; concretes; corrosion; fly ash; reinforcing steels.

INTRODUCTION

The high-volume fly ash (HVFA) concrete incorporates high volumes of fly ash (56 to 58% by mass as cement replacement), and generally has a low water-to-cementitious materials ratio (*w/cm*) of approximately 0.32. The water content is kept at approximately 120 kg/m^3, and the flow slumps are achieved by the use of large dosages of a superplasticizer. The systematic development of the HVFA concrete has progressed for more than a decade. The significant achievement of the research relates to its excellent mechanical properties and long-term durability.[1-4] Some of these properties include:

1. *High long-term compressive strength*—The compressive strengths of over 100 MPa after 10 years have been obtained for HVFA concrete.[5]

2. *High resistance to repeated cycles of freezing and thawing*—The HVFA concrete is highly resistant to the freezing and thawing cycling. A durability factor of > 90% after 1000 cycles has been obtained.[1]

3. *Low permeability*—The HVFA concrete generally exhibits a low value of the total charge in coulombs (generally less than 500 at 90 days) in the ASTM C 1202 test, commonly referred to as the rapid chloride permeability test.[1]

4. *Control of alkali-aggregate reactions*—The HVFA concrete shows no expansion in spite of the highly reactive coarse aggregates used in the concrete mixtures.[1]

Although several studies have been performed on the various aspects of the HVFA concrete, no systematic investigation on the performance of reinforcing steel in HVFA concrete has been previously reported.[6] It is generally believed that the low permeability and high resistivity of the HVFA concrete impedes the oxygen and chloride-ion diffusion into the concrete. This suggests the possibility of a low corrosion rate of steel reinforcement, even through the pH of the pore solution may be somewhat lower than that of the portland cement concrete of equivalent cementitious materials content. The objective of this research is to determine the performance of the commonly used steel reinforcement in HVFA concrete.

SCOPE

In this ongoing investigation, six air-entrained concrete mixtures were made. These included four control portland cement concrete mixtures with *w/c* ranging from 0.32 to 0.76 and the two high-volume fly ash concrete mixtures incorporating ASTM Class F and C fly ashes. Half-cell potential, linear polarization, and AC impedance techniques were applied to monitor the progress of corrosion of the steel reinforcement. A number of slabs, 833 x 600 x 153 mm in size, were cast and ponded with a 3.4% sodium chloride solution. The reinforcing steel bars were placed in the slabs with concrete cover ranging from 13 to 76 mm.

EXPERIMENTAL

Materials

Cement—ASTM Type 1 portland cement was used. Its physical properties and chemical composition are given in Table 1.

Fly ash—Commercially available ASTM Class F fly ash from Point Tupper, Nova Scotia, Canada, and ASTM Class C fly ash from Pleasant Prairie, Wis., were used. Their physical properties and chemical compositions are given in Table 1. The Point Tupper fly ash contains a low calcium content (2.8% of CaO), high iron oxide content (29.9% of Fe_2O_3) and has a specific surface of 236 m^2/kg (Blaine). The Pleasant Prairie fly ash has a CaO content of 28.2% and a specific surface of 422 m^2/kg (Blaine).

Aggregates—The coarse aggregate used was crushed limestone with a maximum nominal size of 19 mm; the fine aggregate was natural sand from the Ottawa region. The coarse and fine aggregates were separated into different size fractions and recombined to a specified gradation as shown in Table 2. The

ACI Materials Journal, V. 96, No. 5, September-October 1999.
Received May 5, 1998, and reviewed under Institute publication policies. Pertinent discussion will be published in the July-August 2000 *ACI Materials Journal* if received by April 1, 2000.

...Institute for Construction, National Research Council of Canada. He is a member of ACI Committee 222, Corrosion of Metals in Concrete. His research interests include multifuctional corrosion-inhibiting admixtures, and corrosion assessment and protection of concrete structures.

J. J. Beaudoin is a principal research officer at the Materials Laboratory of the Institute for Research in Construction. His research interests include the application of AC impedance spectroscopy in cement and concrete structures.

ACI member **Min-Hong Zhang** is a research scientist at the International Centre for Sustainable Development of Cement and Concrete (ICON), CANMET, Ottawa, Canada. She is a member of ACI Committees 213, Lightweight and Aggregate Concrete; 232, Fly Ash and Natural Pozzolans in Concrete; 234, Silica Fume in Concrete; and the International Activities Committee.

ACI honorary member **V. M. Malhotra** is Scientist Emeritus of the International Centre for Sustainable Development of Cement and Concrete (ICON), CANMET. He is a former member of the ACI Board of Direction and is an active member of numerous ACI committees.

Table 1—Physical properties and chemical composition of cement and fly ashes

		ASTM Type I cement	Fly ash	
			ASTM Class F	ASTM Class C
Physical tests				
Specfic gravity		3.15	2.67	2.62
Fineness	Passing 45 μm, %	87.9	90.2	80.0
	Specific surface, Blaine, m^2/kg	388	236	422
	Nitrogen absorption, m^2/kg	—	—	—
Compressive strength of 51 mm cubes, MPa	7-day	33.5	—	—
	28-day	39.7	—	—
Water requirement, %		—	95.0	—
Pozzolanic activity index, %	7-day	—	75.2	94.9
	28-day	—	92.8	101.4
Chemical analyses, %				
Silicon dioxide (SiO_2)		20.6	40.7	33.9
Aluminum oxide (Al_2O_3)		4.0	17.9	19.4
Ferric oxide (Fe_2O_3)		3.1	29.9	6.1
Calcium oxide (CaO)		62.8	2.8	28.2
Magnesium oxide (MgO)		2.6	1.1	4.8
Sodium oxide (Na_2O)		—	0.7	1.9
Potassium oxide (K_2O)		—	1.6	0.4
Equivalent alkali ($Na_2O + 0.658K_2O$)		0.8	1.8	2.1
Phosphorous oxide (P_2O_5)		—	0.2	1.5
Titanium oxide (TiO_2)		—	0.9	1.7
Sulfur trioxide (SO_3)		3.1	1.3	3.0
Loss on ignition		1.8	2.0	0.3
Bogue potential compound composition				
Tricalcium silicate (C_3S)		59.3	—	—
Dicalcium silicate (C_2S)		14.4	—	—
Tricalcium aluminate (C_3A)		5.3	—	—
Tetracalcium aluminoferrite (C_4AF)		9.3	—	—

coarse and fine aggregates each had a specific gravity of 2.70, and water absorption of 0.60 and 0.80%, respectively.

Superplasticizer—A sulfonated, naphthalene-formaldehyde condensate type superplasticizer was used in the concrete mixtures. The superplasticizer is a dark brown color solution containing 42% solids.

Air-entraining admixture—A multicomponent synthetic resin type of air-entraining admixture was used in all the concrete mixtures.

Coarse aggregate		Fine aggregate	
Sieve size, mm	Cumulative percentage retained	Sieve size, mm	Cumulative percentage retained
19.0	0	4.75	0
12.7	35	2.36	10
9.5	60	1.18	32.5
4.75	100	0.60	57.5
—	—	0.30	80
—	—	0.15	94
—	—	Pan	100

Steel reinforcement—Carbon steel reinforcing bars, 15 mm in diameter, were used in the test. Reinforcing steel bars were used as received.

Preparation and properties of concrete specimens

Concrete mixtures—The proportions of the concrete mixtures are summarized in Table 3.

Properties of fresh concrete—The concrete was mixed in a laboratory counter-current mixer for a total of 5 min. The properties of the fresh concrete, including the slump, air content, and unit weight, were determined immediately after mixing, and the results are given in Table 4. The slump and air content of the concrete ranged from 70 to 175 mm, and from 4.8 to 6.0%, respectively. The unit weight and temperature of the fresh concrete ranged from 2285 to 2412 kg/m^3, and 18.5 to 23.0 C, respectively.

Compressive strength—Cylindrical specimens, 100 x 200 mm in size, were also cast, and the compressive strength of the concrete at 7, 28, 91, and 365 days was determined according to ASTM C 39 (Table 5). The compressive strength of the control portland cement concrete at 28 days ranged from 18.4 to 61.1 MPa. The concrete incorporating the Class C fly ash had a 28-day compressive strength of 55.8 MPa, which was slightly lower than that of the control portland cement concrete with a w/c of 0.32 (61.1 MPa). The concrete incorporating the Class F fly ash had a 28-day compressive strength of 36.4 MPa, which was similar to that of the control concrete with a w/c of 0.43 (37.7 MPa).

Resistance to chloride-ion penetration—The resistance of the concrete to the penetration of the chloride ions, measured in terms of the charge passed through the concrete (ASTM C 1202), was determined on two disks cut from the top portion of 100 x 200 mm cylinders cured in a standard moist room for 28 days. The results presented are the averages from two concrete specimens (Table 5). The ASTM guidelines concerning the chloride-ion penetrability are given in Table 6.

Chloride ponding test—One reinforced concrete slab, 333 x 600 x 153 mm in size (Fig. 1), was cast from each concrete mixture and consolidated using an internal vibrator. Four pairs of reinforcing bars were embedded in each concrete slab with concrete covers ranging from 13 to 76 mm, as shown in Fig. 1. The slabs were cured under wet burlap for 7 days, and then exposed to the laboratory air for approximately 50 days. The top surface of the slabs was ponded continuously with a 3.4% sodium chloride solution, and the corrosion progression of the steel reinforcement was assessed using half-cell potential, linear polarization and, AC impedance techniques after 2 and 6 months of the ponding.

ASSESSMENT TECHNIQUES FOR CORROSION OF STEEL REINFORCEMENT

Half-cell potential

The half-cell potential is an indication of the relative probability of corrosion activity, and was determined according to ASTM C 876 with minor differences. In the experiment, $Hg/HgCl_2$ electrode was used instead of the $Cu/CuSO_4$

Mixture no.	Type of fly ash	Fly ash content, %	$w/c + FA$	w/c	Quantities, kg/m³						AEA‡, mL/m³
					Water*	Cement	Fly ash	Fine aggregate	Coarse aggregate	SP†	
N1	Class F	58	0.32	0.76	119	156	217	751	1124	4.0	403
N2	Class C	58	0.32	0.76	119	156	217	747	1120	5.0	403
N3	—	—	0.32	0.32	120	376	0	769	1150	9.1	457
N5	—	—	0.43	0.43	160	372	0	723	1085	0.5	111
N6	—	—	0.55	0.55	165	300	0	736	1099	0.0	60
N4	—	—	0.76	0.76	165	218	0	768	1147	0.0	91

*Including water in superplasticizer.
†Superplasticizer, naphtahlene based.
‡Air-entraining admixture.

Table 4—Properties of fresh concrete

Mixture no.	Type of fly ash	Fly ash content, %	$w/c + FA$	w/c	Temperature, C	Slump, mm	Unit weight, kg/m³	Air content, %
N1	Class F	58	0.32	0.76	23.0	90	2369	5.4
N2	Class C	58	0.32	0.76	22.5	90	2369	5.5
N3	—	—	0.32	0.32	23.0	175*	2412	4.8
N5	—	—	0.43	0.43	—	70	2327	5.2
N6	—	—	0.55	0.55	18.5	75	2285	6.0
N4	—	—	0.76	0.76	20.0	100	2285	5.6

*Concrete mixtures designed to have slump of 100 ± 20 mm. Unfortunately, for control concrete with $w/c = 0.32$, this could not be achieved with addition of 4 to 5 kg/m³ of superplasticizer. Therefore, dosage of superplasticizer had to increase for this concrete. Control concrete with slump of 175 mm appeared to have comparable workability with fly ash concretes.

Table 5—Compressive strength of hardened concrete

Mixture no.	Type of fly ash	Fly ash content, %	$w/c + FA$	w/c	Unit weight, kg/m³	Compressive strength, MPa				Resistance to chloride ion penetration, columbs, 28-day
						7-day	28-day	91-day	365-day	
N1	Class F	58	0.32	0.76	2424	24.6	36.4	46.7	56.7	1440
N2	Class C	58	0.32	0.76	2410	41.0	55.8	60.7	67.9	1395
N3	—	—	0.32	0.32	2450	51.7	61.1	67.1	78.6	1730
N5	—	—	0.43	0.43	2331	35.4	37.7	41.0	48.2	3970
N6	—	—	0.55	0.55	2343	26.5	31.0	33.5	35.7	5250
N4	—	—	0.76	0.76	2304	14.6	18.4	20.7	21.7	5970

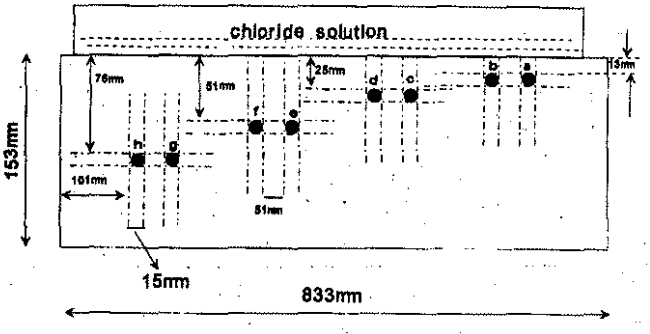

Fig. 1—Reinforcing steel layout of reinforced concrete test slabs.

electrode specified in ASTM C 876. The standard potential of $Cu/CuSO_4$ and $Hg/HgCl_2$ is 340 and 268 mV versus that of hydrogen standard electrode, respectively, and the difference between the two reference electrodes is 72 mV. The guidelines described in ASTM C 876 provide general principles for evaluation of the reinforcing steel corrosion in concrete (Table 7).

Linear polarization

The basic principle of the linear polarization technique to determine the corrosion rate of each reinforcing bar embedded in concrete is to apply a slow potential scan close to the corrosion potential Φ_{corr} and to record polarization current I. The polarization resistance R_p of the reinforcing steel is defined as the slope of a potential-current density plot at the corrosion potential Φ_{corr}

$$R_p = \left(\frac{\Delta V}{\Delta I}\right)\Phi_{corr} \quad (1)$$

where ΔV and ΔI are applied potential and current response, respectively. The corrosion current density is calculated from the Stern-Geary equation[7]

$$I_{corr} = \frac{B}{R_p} \text{ and } B = \frac{\beta_a\beta_c}{2.303(\beta_a + \beta_c)} \quad (2)$$

where B is the so-called Stern-Geary constant that can be determined by a mass loss experiment and β_a and β_b are the Tafel slopes for the anodic and cathodic reactions, respectively. Values of B between 13 and 52 mV are often used. For example, 50 mV was used by John et al.[8] and 35 mV by Wenger and Galland.[9] Andrade and Gonzales[10] suggested a value of 26 or 52 mV to be used in the calculation for the bare steel in the active and passive stages, respectively. The calculated R_p may

Charge passed, coulombs	Chloride-ion penetrability
> 4000	High
2000 to 4000	Moderate
1000 to 2000	Low
100 to 1000	Very low
< 100	Negligible

Table 7—General guidelines for half-cell potential data interpretation

Half-cell potential reading versus $Cu/CuSO_4$ (ASTM C 876)	Half-cell potential reading versus $Hg/HgCl_2$ (used in experiment)*	Corrosion activity
Less negative than −200 mV	Less negative than −128 mV	90% probability of no corrosion
Between −200 and −350 mV	Between −128 and −278 mV	Corrosion activity uncertain
More negative than −350mV	More negative than −278 mV	90% probability of corrosion

*Standard potential of $Cu/CuSO_4$ and $Hg/HgCl_2$ is 340 and 268 mV that of hydrogen standard electrode, respectively. Difference of two reference electrodes is 72 mV.

Table 8—Guideline for estimation of corrosion extent using I_{corr}

Corrosion current density, μA/cm²*	Corrosion rate, μA/m†	Extent of corrosion
$I_{corr} < 0.1$	< 47	P: passive condition
$0.1 < I_{corr} < 0.5$	47 < C. R. < 235	L: low to moderate corrosion
$0.5 < I_{corr} < 1$	235 < C. R. < 470	M: moderate to high corrosion
$I_{corr} > 1$	> 470	H: high corrosion

*From Reference 13.
†1 m of No. 5 reinforcing bar (diameter of 15 mm) has geometrical area of 470 cm².

have an inherent error of approximately 200% as the B constant varies between 13 and 52 mV.

The corrosion current density was measured on each reinforcing bar embedded in the concrete slabs. The electrochemical measurements were made using an EG&G potentiostat model 6310, and the $Hg/HgCl_2$ reference electrode was used. Polarization experiments were performed at a scan rate of 0.1 mV/s (ASTM G59 recommends a scan rate of < 0.1667mV/s). They were initiated at 20 mV below the corrosion potential and terminated at a maximum of 20 mV above the corrosion potential. The IR drop can be corrected for ($R_p = \Delta V / I_{measured} - R_c$) using the concrete resistance obtained from the impedance measurement. However, in this study, the correction was insignificant due to the small current.

AC Impedance

The AC impedance measurements were carried out using a SI 1255 HF frequency response analyzer and a SI 1286 electrical interface. A small sinusoidal voltage signal of 30 mV was applied over the range of frequencies 75 kHz to 0.05 Hz. The current response caused by the voltage perturbation was measured as well as the phase shift of the current and voltage characteristics. A three-electrode configuration was used.

The corrosion resistance of the reinforcing bars was estimated through an equivalent circuit fitting analysis of the AC impedance spectra. This equivalent circuit consists of three parallel combinations of a pure resistor and a frequency dependent capacitor (Fig. 2). The latter is called a constant phase element,[11] $C = C_o(j\omega)^{-\alpha}$ (C_o is a constant and equal to the capacitance of a pure capacitor), introduced to account for the shape of the depressed complex plot. The three resistor/capacitor circuits represent the concrete matrix, interface film and steel surface corrosion processes, respectively. The detailed R_p determination procedure is given elsewhere.[12] The corrosion current density was calculated by knowing the polarization resistance R_p determined through a computer equivalent circuit simulation and using the Stern-Geary equation. A B value of 26 mV for active corrosion, and the R_p values obtained from the impedance spectra fitting were applied in the calculation.

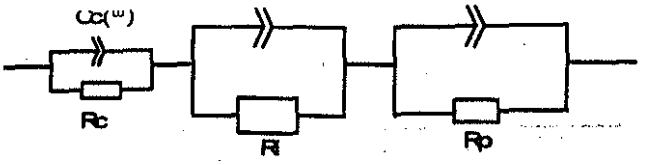

Fig. 2—Equivalent circuit used in AC impedence fitting process consisting of three parallel combinations of pure resistor and frequency dependent capacitor. Note: R_c and C_c = concrete resistance and matrix solid/liquid interface capacitance; R_i and C_i = steel/concrete interface film resistance and capacitance; and R_p and C_{dl} = steel polarization resistance and double-layer capacitance.

A guideline for the estimation of corrosion extent using corrosion current density is given in Table 8.[13]

RESULTS AND DISCUSSION

Resistance to chloride-ion penetration (ASTM C 1202)

The HVFA concretes had higher resistance to chloride-ion penetration than the control portland cement concrete as indicated by ASTM C 1202 test. The accumulated charge passed at 28 days was 1440 and 1395 coulombs for the HVFA concrete incorporating ASTM Class F and Class C fly ash, respectively. These values were lower than 1730 coulombs for the control concrete with a w/c of 0.32. According to ASTM C 1202, concrete with a value of less than 1000 coulombs is considered to have an excellent resistance to the penetration of chloride ions. Other published data on the investigations dealing with HVFA concrete show that the values of the charge passed through concrete decrease dramatically with age, and values as low as about 250 coulombs have been reported for tests performed on the HVFA concretes at 91 days.[1]

Electrochemical measurement

Half-cell potential of steel reinforcement in concrete slabs—The half-cell potential or corrosion potential is often used as an indication of the relative probability of the corrosion activity. The data analysis guidelines described in ASTM C 876 provide general principles for the evaluation of the reinforcing steel corrosion in concrete. Generally, the more negative potential readings are associated with the higher probability of the reinforcing steel corrosion. This approximation is quite accurate when chloride ions are present.

The half-cell potentials at the reinforcing bars in the two HVFA concrete slabs and the four control portland cement concrete slabs, measured after 2 and 6 months of ponding with a 3.4% sodium chloride solution, are given in Fig. 3(a) and (b). The letters *a, b, c, d, e, f, g,* and *h* represent the concrete cover to the reinforcing steels of 13, 25, 51, and 76 mm, respectively. The half-cell potential readings obtained from the reinforcing steels embedded in the HVFA concretes and the control concrete with a w/c of 0.32 are relatively noble with values less negative than −100 mV. These readings indicate low probability of the reinforcing steel corrosion. However, the first two reinforcing bars *a* and *b* with a cover thickness of 13 mm embedded in the control concrete with $w/c \geq 0.43$ depicted much more negative half-cell

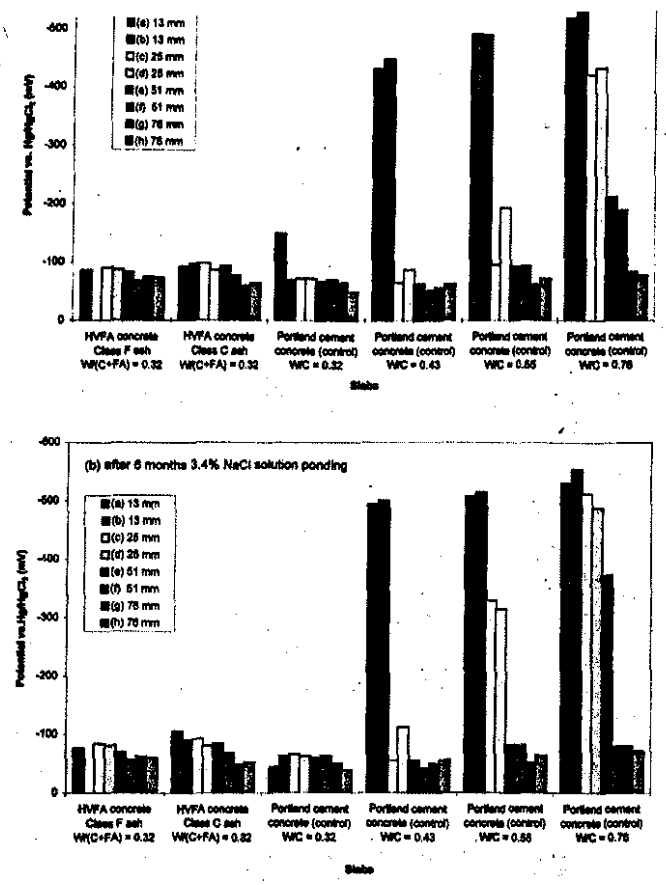

Fig. 3—Half-cell potentials of two HVFA concrete slabs (N1 and N2) and four control slabs (N3 to N6) measured after: (a) 2 months; and (b) 6 months of sodium chloride solution ponding.

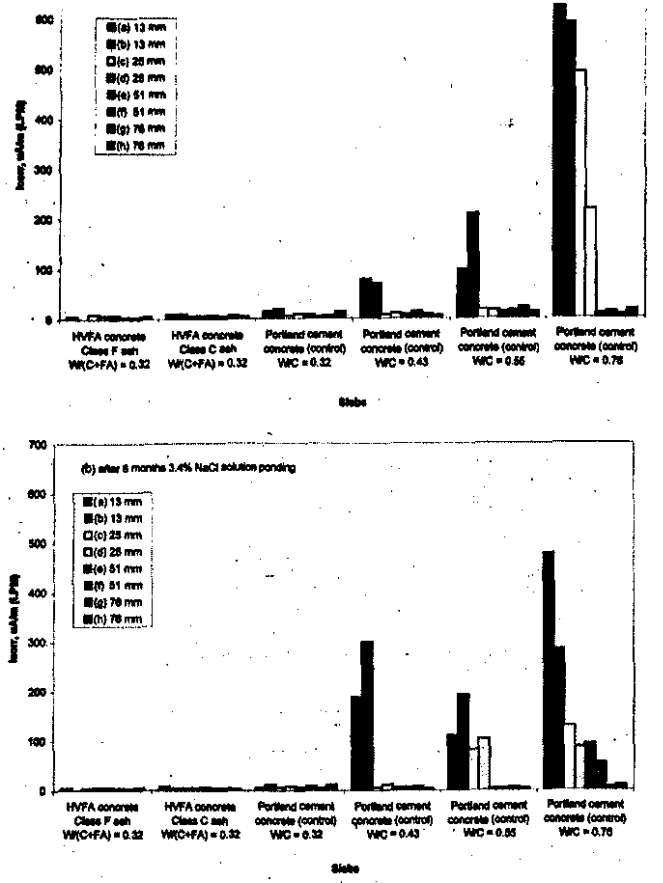

Fig. 4—Corrosion rate I_{corr} obtained by linear polarization technique of two HVFA concrete slabs (N1 and N2) and four control slabs (N3 to N6) measured after: (a) 2 months; and (b) 6 months of sodium chloride solution ponding. (Note: I_{corr} values for reinforcing bars with 13 and 25 mm concrete covers of control concrete slab with a w/c of 0.76 obtained after 2 months of ponding with sodium chloride solution were higher than those obtained after 6 months of ponding with solution. Behavior may be attributed to accumulation of corrosion products. When chloride-induced corrosion takes place on surface of steel reinforcement, I_{corr} could be high initially as elelctrochemical reaction [$Fe = Fe^{+2} + 2e^-$] favored to oxidation of Fe. Reaction will decline, however, as the Fe^{+2} ion concentration increases, leading to increase of reverse reaction [Fe reduction] and decrease of I_{corr}.)

potential values (< −300 mV) even after 2 months of ponding. After 6 months of ponding, the reinforcing bars with 25 and 51 mm concrete cover in the concrete slab with a *w/c* of 0.76, and with 25 mm concrete cover in the concrete slab with a *w/c* of 0.55 showed the potential values more negative than −300 mV. These observations indicated a high probability of corrosion of the corresponding reinforcing bars.

Corrosion current determined using linear polarization technique—The linear polarization technique is a useful, nondestructive, relatively fast, cost-effective, and quantitative approach for corrosion assessment of reinforced concrete. The unit of the corrosion rate is normally expressed by $\mu A/cm^2$ or mA/m^2. As it is difficult to determine accurate reinforcing bar surface area, it may be more appropriate to use the unit length instead of the unit area to represent the reinforcing steel corrosion rate. Therefore, a unit of $\mu A/m$, meaning the corrosion current density of a meter-long reinforcing steel bar, is used in the discussion that follows.

Fig. 4(a) and (b) illustrate the corrosion rate I_{corr} obtained by the linear polarization technique of the two HVFA concrete slabs (N1 and N2) and the four control portland cement concrete slabs (N3 to N6). The measurements were carried out after 2 and 6 months of ponding with the chloride solution. The values of the I_{corr} for all the reinforcing bars in HVFA concrete slabs were less than 15 $\mu A/m$ regardless of the concrete cover even after 6 months. This indicated that the HVFA concrete had excellent resistance against chloride-ion penetration. Similar results were observed in the control portland cement concrete with a *w/c* of 0.32. In contrast, the I_{corr} values were much higher for the reinforcing bars with 13 and 25 mm concrete cover in the control concrete slab with a *w/c* of 0.76, and for reinforcing bars with 13 mm concrete cover in the control concrete slabs with *w/c* of 0.43 and 0.55, even after 2 months of ponding (Fig. 4(a)). Corrosion progression was clearly observed in control portland cement concrete slabs with *w/c* of 0.55 and 0.76. The reinforcing bars with 51 mm concrete cover in control concrete with a *w/c* of 0.76 and those with 25-mm concrete cover in control concrete with a *w/c* of 0.55 showed significant increases in the corrosion rate after 6 months of ponding with the 3.4% chloride solution. These observations are in good agreement with the half-cell potential results.

Corrosion current determined using AC impedance technique—The rates of corrosion of the reinforcing bars in the six concrete slabs were also determined using the AC impedance technique. An equivalent circuit fitting of the experimental impedance spectra procedure was applied to estimate the value of the polarization resistance R_p. A typical example of the experimental data fitting using the electrical equivalent circuit models, as described in Fig. 2, is presented in the plots of real versus imaginary (Fig. 5(a)), phase angle versus log (frequency) (Fig. 5(b)), and log (modulus) versus log (frequency) (Fig. 5(c)). The circles represent the experimental data, and the solid

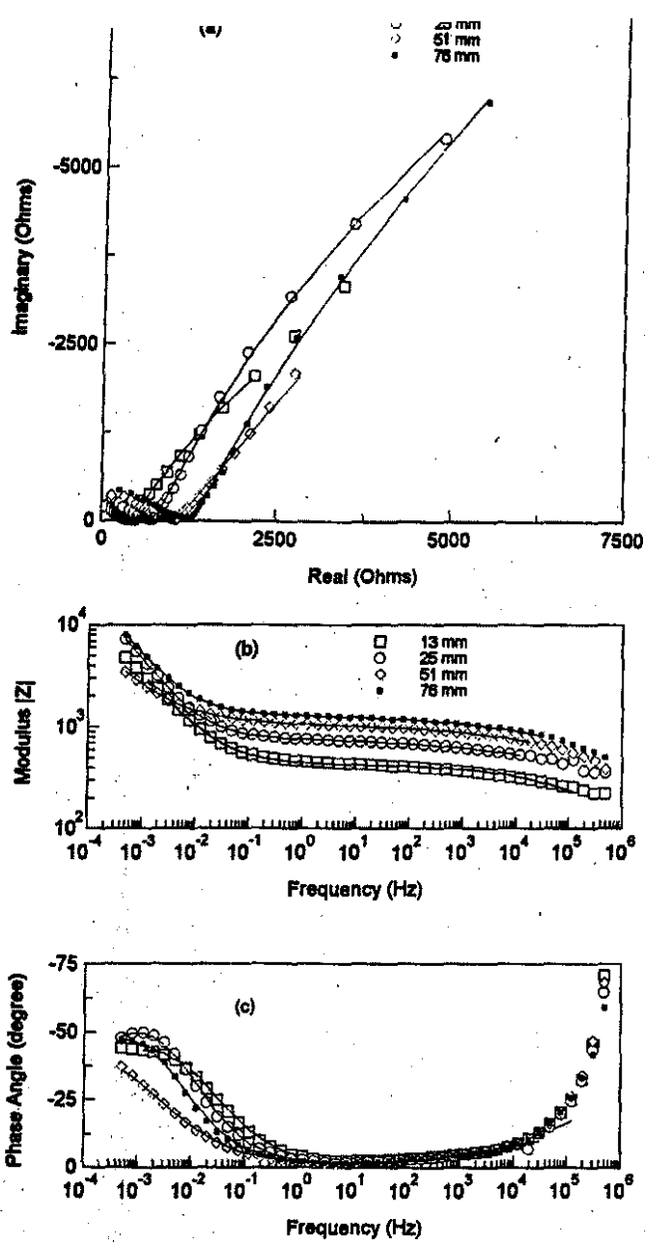

Fig. 5—Typical example (recorded from N1 after 2 month ponding with 3.4% sodium chloride solution) of the experimental data fitting using the electrical equivalent circuit (Fig. 2) is presented in plots of: (a) real versus imaginary; (b) log (modulus) versus log (frequency); and (c) phase angle versus log (frequency).

lines the computer fitting results. Two partial arcs were observed in the real versus imaginary plot. These arcs are associated with the concrete matrix and the steel surface corrosion process (the steel/concrete interface film was not observed). Good agreement was obtained between the circles and the solid line, as can be seen in Fig. 5(a) to (c). The values of R_p were determined using this best-fit approach.

Fig. 6(a) and (b) display the corrosion rate of the reinforcing bars I_{corr} in the two HVFA concrete slabs (N1 and N2) and the four control portland cement concrete slabs (N3 to N6) after 2 and 6 months ponding with the chloride solution, respectively. These results were consistent with those obtained by the linear polarization technique. The values of I_{corr} were very low (< 7.5 μA/m) for all the reinforcing bars embedded in the HVFA concrete slabs and the control concrete slab with a w/c of 0.32. However, the values of I_{corr} were significantly higher for all the reinforcing bars with 13 mm concrete cover in control concrete slabs with $w/c \geq 0.43$ and for those with 25 mm cover in control concrete with w/c of 0.55 and 0.76. Even one of the reinforcing bars with 51 mm cover in the control concrete with a w/c of 0.76 showed very high corrosion current after 6 months.

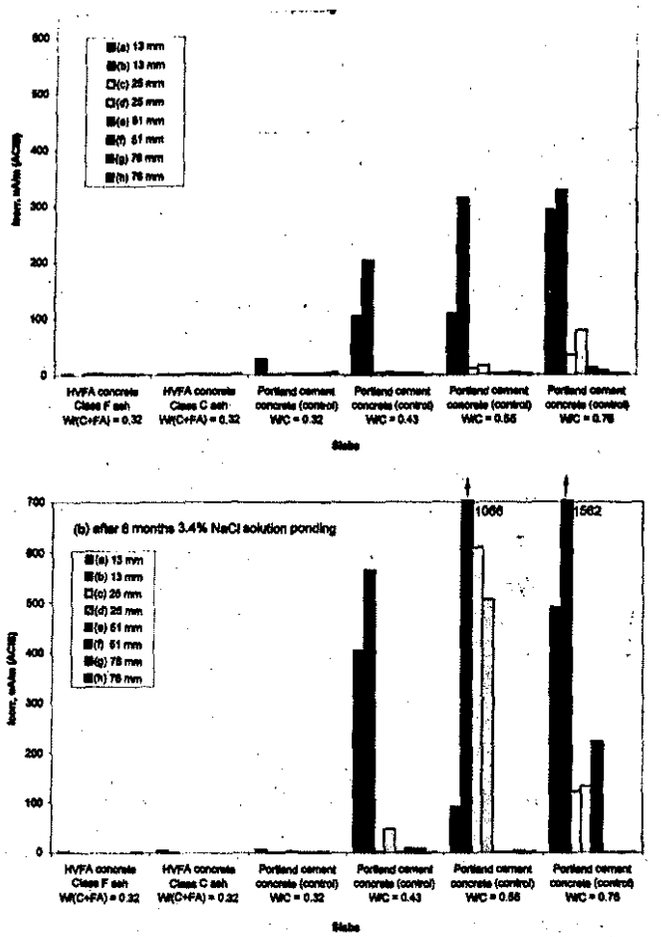

Fig. 6—Corrosion rate I_{corr} obtained by AC impedance technique of two HVFA concrete slabs (N1 and N2) and four control slabs (N3 to N6) measured after: (a) 2 months; and (b) 6 months of sodium chloride solution ponding.

Comparison of results obtained by three electrochemical techniques—The results obtained by the half-cell potential, linear polarization, and AC impedance techniques are in good agreement. More negative half-cell potential readings were associated with larger corrosion current determined by both the AC impedance and linear polarization techniques.

The plots of the half-cell potential versus logarithmic corrosion rate determined by the linear polarization and AC impedance techniques are given in Fig. 7(a) and (b), respectively. A linear trend for the potential-log (I_{corr}) relation appears to exist. The I_{corr} data obtained by the linear polarization method exhibit less scattering than those obtained by the AC impedance. In fact, the linear relationship between corrosion potential and log (I_{corr}) exists theoretically in the chloride-induced corrosion.[14]

A comparison of the I_{corr} values obtained by the linear polarization and AC impedance techniques in a log-log plot is presented in Fig. 8. A solid reference line is shown to indicate a linear trend between the two measurements. It appears that both techniques are in a relatively good agreement with respect to I_{corr} values when the reinforcing steel is under active corrosion. The AC impedance technique, however, tends to give lower I_{corr} values when the reinforcing steel are in a passive state.

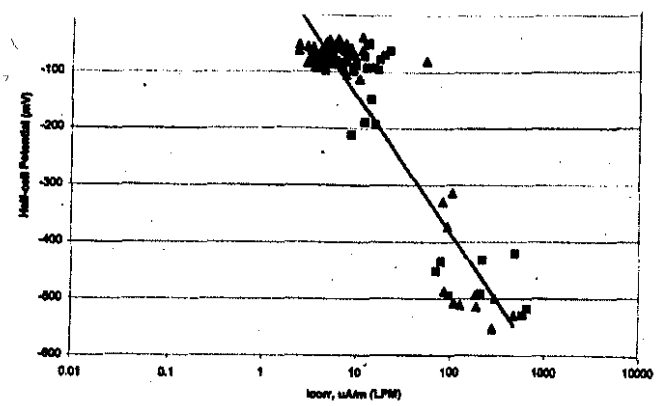

(a)

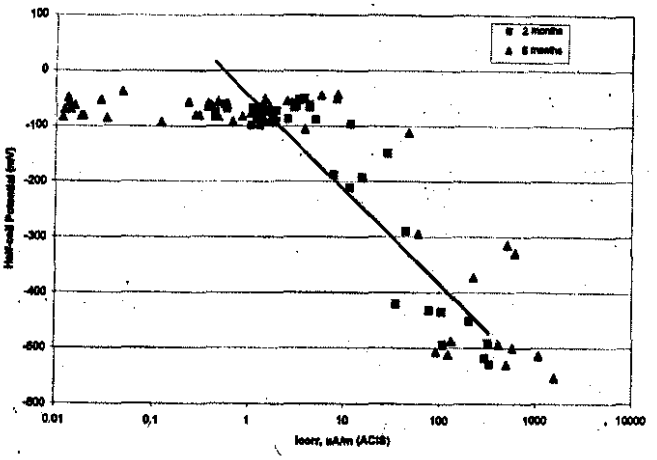

(b)

Fig. 7—Plots of half-cell potential versus logarithmic corrosion rate determined by: (a) linear polarization; and (b) AC impedance techniques.

Corrosion of steel reinforcement in concrete—The concrete cover is a physical barrier that impedes the chloride-ion penetration, thus protecting the reinforcing steel from corrosion. Good quality and appropriate depth of concrete cover can significantly influence the rate of carbonation, and the diffusion of corrosion-inducing species into the concrete-steel interface region. The thicker this cover is, the longer it takes for the chloride ions to reach the surface of reinforcing steel. A greater protection against corrosion is therefore assured.

The corrosion conditions of the steel reinforcement in the six reinforced concrete slabs were evaluated after 6 months of the chloride ponding. Table 9(a) summarizes the corrosion probability of steel reinforcements by means of half-cell potential according to ASTM Standard C 876. The HVFA concretes and the control concrete with a w/c of 0.32 showed no probability of corrosion even on the steel reinforcing bars with 13 mm concrete cover. The excellent performance of steel reinforcement in HVFA concrete is due to the very low permeability of the concrete.[15] For all other control concretes with $w/c \geq 0.43$, the first two reinforcing steel bars with 13 mm cover depicted high probability of corrosion. For concrete with a w/c of 0.76, even the reinforcing bars with 25 mm cover showed high probability of corrosion.

Table 9(b) and 9(c) give a summary of the corrosion conditions of the steel reinforcement in the six concrete slabs evaluated by the linear polarization and the AC impedance techniques, respectively. It is clear that the HVFA concretes and the control concrete with a w/c of 0.32 provided adequate protection to the reinforcing steel from corrosion in terms of mitigating the chloride-ion penetration. Higher corrosion currents were observed for the steel reinforcing bars embedded in the control concrete with $w/c \geq 0.43$. As expected, the poorest performance was of the reinforcing bars in the control concrete with a w/c of 0.76 where corrosion of the reinforcing steel was detected even with 51 mm concrete cover. Significant corrosion of reinforcing steel with 13 mm cover was also found in other control concrete slabs with w/c of 0.43 and 0.55 after 6 months ponding with the chloride solution. The results confirmed the evaluation by the half-cell potential measurement.

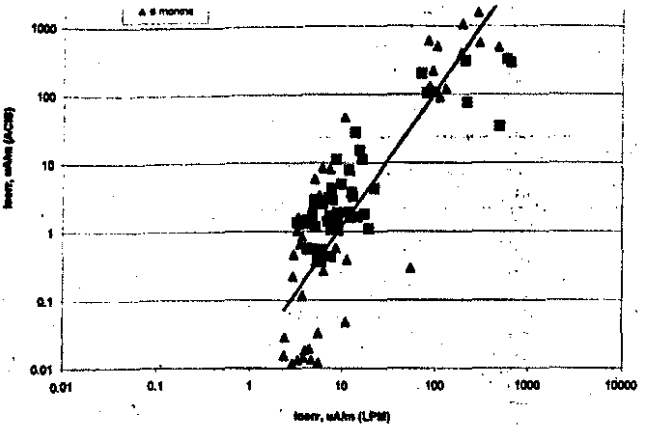

Fig. 8—Log-log plot of I_{corr} values obtained by both linear polarization (LPM) and AC impedance (ACIS) techniques.

Table 9(a)—Probability of corrosion after 6 months evaluated by half-cell potential method

No.	Concrete mixture	13 mm	25 mm	51 mm	76 mm
N1	HVFA concrete, Class F ash, $w/(c + FA) = 0.32$	Low	Low	Low	Low
N2	HVFA concrete, Class C ash, $w/(c + FA) = 0.32$	Low	Low	Low	Low
N3	Control portland cement concrete, $w/c = 0.32$	Low	Low	Low	Low
N5	Control portland cement concrete, $w/c = 0.43$	High	Low	Low	Low
N6	Control portland cement concrete, $w/c = 0.55$	High	High	Low	Low
N4	Control portland cement concrete, $w/c = 0.76$	High	High	Middle	Low

Note: Low = half-cell potential less negative than −128 mV, indicating 90% probability of no corrosion; Middle = half-cell potential between −128 and −278 mV, indicating corrosion activity is uncertain; and High = half-cell potential more negative than −278 mV, indicating 90% probability of corrosion.

Table 9(b)—Severity of corrosion after 6 months evaluated by linear polarization technique

No.	Concrete mixture	13 mm	25 mm	51 mm	76 mm
N1	HVFA concrete, Class F ash, $w/(c + FA) = 0.32$	P	P	P	P
N2	HVFA concrete, Class C ash, $w/(c + FA) = 0.32$	P	P	P	P
N3	Control portland cement concrete, $w/c = 0.32$	P	P	P	P
N5	Control portland cement concrete, $w/c = 0.43$	M	P	P	P
N6	Control portland cement concrete, $w/c = 0.55$	L	L	P	P
N4	Control portland cement concrete, $w/c = 0.76$	M	L	L	P

Note: P = passive; L = low; and M = moderate.

No.	Concrete mixture	13 mm	25 mm	51 mm	76 mm
N1	HVFA concrte, Class F ash, $w/(c + FA) = 0.32$	P	P	P	P
N2	HVFA concrete, Class C ash, $w/(c + FA) = 0.32$	P	P	P	P
N3	Control portland cement concrete, $w/c = 0.32$	P	P	P	P
N5	Control portland cement concrete, $w/c = 0.43$	H	P	P	P
N6	Control portland cement concrete, $w/c = 0.55$	H	H	P	P
N4	Control portland cement concrete, $w/c = 0.76$	H	L	L	P

Note: P = passive; L = low; and H = high.

CONCLUSIONS

The HVFA concretes had higher resistance to chloride-ion penetration than the control portland cement concrete as indicated by ASTM C 1202 test.

The performance of the reinforcing steel bars in the high-volume fly ash concretes after 6 months of ponding with a 3.4% sodium chloride solution was excellent. There was no significant steel corrosion taking place on the reinforcing steel embedded in the HVFA concrete even with 13 mm concrete cover. This performance of the HVFA concrete is equivalent to that of the control concrete with a w/c of 0.32, and is better than the control concrete with $w/c \geq 0.43$.

Significant corrosion rates were observed for the reinforcing steel embedded in control portland cement concrete with $w/c \geq 0.43$. As expected, the poorest performance was of the control concrete with a w/c of 0.76, where corrosion of reinforcing steel was detected, even with 51 mm concrete cover.

ACKNOWLEDGMENTS

Grateful acknowledgment is made to Electric Power Research Institute (EPRI) of Palo Alto, Calif., for funding of the project. Thanks are due to Nathalie Chagnon, Bruce Baldock, Glendon Pye and Bob Myers of NRC/IRC, and R. Chevrier and A. Ferro of CANMET for their help with experimental work.

REFERENCES

1. Bilodeau, A.; Sivasundaram, V.; Painter, K. E.; and Malhotra, V. M., "Durability of Concrete Incorporating High-Volume Fly Ash from Sources Strength Development of High-Volume Fly Ash Concrete," *Cement and Concrete Composites*, V. 12, 1990, pp. 263-270.

3. Feldman, R. F.; Garette, G. G.; and Malhotra, V. M., "Studies on Mechanism of Development of Physical and Mechanical Properties of High-Volume Fly Ash Cement Pastes," *Cement and Concrete Composites*, V. 12, 1990, pp. 245-251.

4. Berry, E. E.; Hemmings, R.; and Cornelius, B. J., "Mechanisms of Hydration Reactions in High Volume Fly Ash Pastes and Mortars," *Cement and Concrete Composites*, V. 12, 1990, pp. 253-261.

5. "Investigation of the Long-Term Characteristics of High-Performance Concrete," *Report* by Trow Consulting Engineers, Ltd., under CANMET contract 23440-7-1009/001/SQ, Mar. 1998.

6. Malhotra, V. M., and Ramezanianpour, A. A., "Fly Ash in Concrete," *CANMET/Natural Resources Canada*, CANMET, MSL 94-45(IR), 2nd revised edition, 1994, 297 pp.

7. EG&G, "Linear Polarization," *Princeton Applied Research Application Note-140*, and *Note-148*, "Tafel Plot."

8. John, D. E.; Searson, P. C.; and Dawson, J. L., "Use of AC Impedance Technique in Studies on Steel in Concrete in Immersed Conditions," *British Corrosion Journal*, V. 16, 1981, pp. 102-106.

9. Wenger, F., and Galland, J., "Analysis of Local Corrosion of Large Metallic Structures or Reinforced Concrete Structures by Electrochemical Impedance Spectroscopy," *Electrochimica Acta*, V. 35, 1990, pp. 1573-1578.

10. Andrade, C., and Gonzales, J. A., "Quantitative Measurements of Corrosion Rate of Reinforcing Steels Embedded in Concrete Using Polarization Resistance Measurements," *Werkstoffe und Korrosion*, V. 29, 1978, pp. 515-519.

11. Cole, K. S., and Cole, R. H., "Dispersion and Absorption in Dielectrics, I: Alternating Current Characteristics," *Journal of Chemical Physics*, V. 9, 1941, pp. 341-351.

12. Gu, P.; Elliott, S.; Hristova, R.; Beaudoin, J. J.; Brousseau, R.; and Baldock, B., "A Study of Corrosion Inhibitor Performance in Chloride Contaminated Concrete by Electrochemical Impedance Spectroscopy," *ACI Materials Journal*, V. 94, No. 5, Sept.-Oct. 1997, pp. 385-395.

13. Broomfield, J. P., "Assessing Corrosion Damage on Reinforced Concrete Structures," *Corrosion and Corrosion Protection on Steel in Concrete*, V. 1, Proceedings of International Conference, University of Sheffield, UK, R. N. Swamy, ed., 1994, pp. 1-25.

14. Gu, P.; Beaudoin, J. J.; Tumidajski, P. J.; and Mailvaganam, N. P., "Electrochemical Incompatibility of Patches in Reinforced Concrete," *Concrete International*, V. 19, No. 8, Aug. 1997, pp. 68-72.

15. Bilodeau, A.; Sivasundaram, V.; Painter, K. E.; and Malhotra, V. M., "Durability of Concrete Incorporating High Volumes of Fly Ash from Sources in U.S.," *ACI Materials Journal*, V. 91, No. 1, Jan.-Feb. 1994, pp. 3-12.